Strong localization in conducting Langmuir–Blodgett films of quasi-one-dimensional charge-transfer complexes

ARTICLE *in* SOLID STATE COMMUNICATIONS · AUGUST 2003

Impact Factor: 1.9 · DOI: 10.1016/S0038-1098(03)00459-9

Available online at www.sciencedirect.com
SCIENCE DIRECT®
PERGAMON
Solid State Communications 127 (2003) 577–582
solid state communications
www.elsevier.com/locate/ssc

Strong localization in conducting Langmuir–Blodgett films of quasi-one-dimensional charge-transfer complexes

L.A. Galchenkov, S.N. Ivanov, I.I. Pyataikin*, V.P. Chernov

Institute of Radio Engineering and Electronics, Russian Academy of Sciences, Mokhovaya 11, Building 7, Moscow 125009, Russia

Received 24 October 2002; received in revised form 13 May 2003; accepted 30 May 2003 by P. Sheng

Abstract

The temperature dependence of intragrain conductivity of the Langmuir–Blodgett (LB) films of $(C_{16}H_{33}–TCNQ)_{0.4}(C_{17}H_{35}–DMTTF)_{0.6}$ has been studied by means of measuring the surface acoustic waves (SAW) attenuation in a piezocrystal resonator covered by the LB film. [$(C_{16}H_{33}–TCNQ)_{0.4}(C_{17}H_{35}–DMTTF)_{0.6}$ denotes the surface-active charge-transfer complex of hexadecyltetracyanoquinodimethane ($C_{16}H_{33}–TCNQ$) and heptadecyldimethyltetrathiofulvalene ($C_{17}H_{35}–DMTTF$)]. We have found that the intragrain conductivity decreases with decreasing temperature, following $\sigma \propto \exp(-1/T^{1/2})$ law. According to the theory of electron transport in quasi-one-dimensional disordered systems (Q1D DS) proposed by E.P. Nakhmedov et al. [Sov. Phys. Solid State 31 (1989) 368] and developed by Z.H. Wang et al. [Phys. Rev. B 43 (1991) 4373], this temperature behaviour of the conductivity points to the disorder-induced electron localization within the film grains. Fitting our experimental data to the relations proposed in these references, allowed us to evaluate the electron relaxation times due to scattering by phonons and impurities. Based on structural parameters of the conducting bilayer, we have also estimated the Fermi velocity and density of states at the Fermi level, which enabled us to determine the mean free path and localization length in the film studied.

PACS: 73.61.Ph; 72.80.Le; 73.20.Dx; 68.18. + p

Keywords: A. Thin films; D. Electronic states (localized); D. Electronic transport; E. Ultrasonics

The Langmuir–Blodgett technique is now intensively studied, since it provides a possibility of organizing electron donor and acceptor molecules at the molecular level and producing charge-transfer complexes in the form of ultrathin films suitable for utilization in molecular-scale devices [1]. For the last decade considerable progress in preparation of the films with high conductivity has been achieved. The LB films based on the electron donor bis(ethylenedioxy)tetrathiafulvalene (BEDO-TTF) in combination with various acceptors exhibit the highest conductivity among the films of charge-transfer complexes. For example, the room-temperature conductivity of the films of the mixture of $(BEDO\text{-}TTF)_{0.71}(C_{10}H_{21}–TCNQ)_{0.29}$ with eicosanoic acid is about 10 S/cm [2], and the conductivity of the films of the mixture of BEDO-TTF with behenic acid reaches 40 S/cm [3], the highest known number at present. However, the LB film conductivity is still several times less than the one of the corresponding bulk crystals [for example, the crystals of $(BEDO\text{-}TTF)ReO_4{\cdot}(H_2O)$ have a room-temperature conductivity of $\approx$147 S/cm [4]]. The relatively low conductivity found in LB films, compared with bulk parent crystals, reduces significantly the area of possible applications of these films in molecular electronics.

Two main causes that reduce the film conductivity have been identified at present. The first one is the granular structure of the films and, as a result, the presence of intergrain potential barriers causing thermally activated tunneling transport through grain boundaries. The second cause is significant difference in the mechanism of the intragrain conductivity itself, compared to the one observed in the bulk parent crystals. To improve the film conductivity, a more detailed study of the intragrain conductivity is needed. Furthermore, new physical phenomena may be probably observed in such study because of the reduced

* Corresponding author. Tel.: +7-95-203-8414; fax: +7-095-203-8414.
E-mail address: iip@mail.cplire.ru (I.I. Pyataikin).

0038-1098/03/$ - see front matter © 2003 Elsevier Ltd. All rights reserved.
doi:10.1016/S0038-1098(03)00459-9

dimensionality of the LB films. For example, the electrical transport mechanism of the films could have several features that are not observed in the corresponding bulk crystals.

The study of the LB film conductivity at the intragrain level was begun by Barraud with co-workers [5]. They used a microwave-cavity perturbation technique, which proved itself to be a powerful tool for studying conductivity of the bulk organic conductor crystals [6,7]. Unfortunately, applying this technique to LB films encounters a serious difficulty, since the films cannot be produced in free-standing form, and the microwave field perturbation caused by the substrate with thickness of about 0.5 mm, exceeds the one caused by the LB film with thickness of 300–500 Å by many orders of magnitude. So, to obtain acceptable accuracy of the measurements it is necessary to provide high stabilities of the driving generator frequency and experimental setup parameters during the process of measurements. These circumstances determine the accuracy of the measurements and the width of the accessible temperature range.

Previously [8], we have applied another approach to the study of the temperature dependence of the intragrain conductivity of the films, based on measuring the surface acoustic waves (SAW) attenuation in a piezocrystal resonator covered by the LB film. In Ref. [8] we have shown that the SAW attenuation is determined by the film conductivity and directly proportional to the SAW frequency. Furthermore, the attenuation caused by the film exceeds the one induced by intrinsic losses in the resonator material ($LiNbO_3$) by 1–1.5 order of magnitude (depending on the SAW frequency). Hence, it appears that measuring the temperature dependence of the intragrain conductivity of the films using this technique is much more simple, and not a less accurate procedure than using the cavity perturbation technique.

In this article, we present results of SAW technique measurements of the intragrain conductivity of the LB films of the charge-transfer complex $(C_{16}H_{33}–TCNQ)_{0.4}(C_{17}H_{35}–DMTTF)_{0.6}$ as a function of temperature. The intragrain conductivity was found to follow $\sigma \propto \exp(-1/T^{1/2})$ law, indicating that the electron states in the TCNQ chains within the film grains are localized. The observed temperature dependence of the conductivity agreed qualitatively and quantitatively with the predictions of the theory of electron localization in Q1D DS proposed in Ref. [9] and developed in Ref. [10]. The fit of the theoretical relations derived in these references to our experimental data allowed us to extract the electron relaxation times due to scattering by phonons and impurities, the mean free path and localization length in our film. The structure of the films studied and charge transport mechanism in them are typical for conducting LB films of the Q1D charge-transfer complexes. As a result, all the discussed conduction mechanism peculiarities here caused by electron localization are common for this class of conducting LB films.

A detailed description of LB film deposition onto $LiNbO_3$ resonators, measuring the acoustic attenuation and calculating the film conductivity from the attenuation data was presented by us in Ref. [8]. The deposition of the films onto contact structures for two-terminal dc conductivity measurements was performed simultaneously with the film deposition onto the resonators. Several resonators with fundamental frequencies ranging from 30 to 150 MHz were measured with similar results. All data shown in this article are obtained using a single typical resonator with fundamental frequency of 87.9 MHz.

Fig. 1 shows the temperature dependences of the film conductivity measured using the SAW technique (data set 1) and usual dc technique (data set 2). As can be seen, the dc conductivity decreases with decreasing temperature, following the Arrhenius law $\sigma \propto \exp(-T_a/T)$, $T_a \approx 1200$ K, while the conductivity measured by the acoustic technique decays in a less steep manner following $\sigma \propto \exp(-1/T^{\gamma})$ law ($0 < \gamma < 1$). The value of the activation energy, T_a, coincides with the one obtained previously using a four-probe technique [11]. It is widely supposed [1] that the activation character of the dc conductivity of the LB films is due to their granular (2D-polycrystalline) structure: the film consists of randomly oriented grains and the charge carriers contributing to the electrical conductivity need to overcome the intergrain potential barriers whose height determines the activation energy, T_a.

The acoustic technique, unlike the dc one, allows us to measure the intragrain conductivity of the films. Indeed, as it was shown in Ref. [8], the SAW attenuation in a piezocrystal resonator covered by conducting LB film is determined by ohmic losses, caused by the coupling of

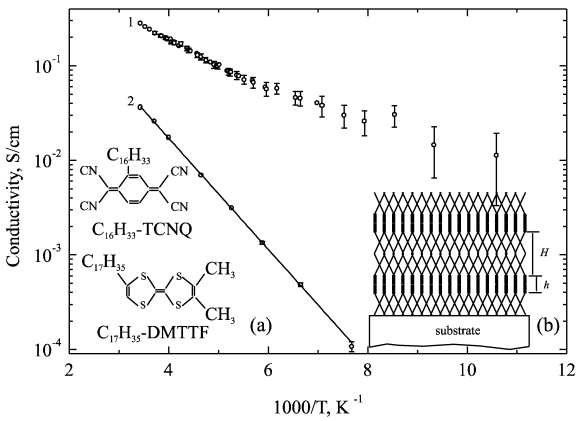

Fig. 1. The temperature dependences of the LB film conductivity measured using the SAW attenuation technique (data set 1) and dc technique (data set 2). A best fit to the dc conductivity data is the function $\sigma \propto \exp(-T_a/T)$, where $T_a \approx 1200$ K. Inset (a) shows the materials used in this study. Inset (b) shows schematic representation of the cross section of the LB film consisting of four monolayers. The conducting bilayers with thickness $h \approx 10$ Å are formed by the TCNQ and DMTTF head groups, the nonconducting bilayers with thickness $H \approx 25$ Å are formed by the $–C_{16}H_{33}$ and $–C_{17}H_{35}$ side groups.

high-frequency (10^7–10^9 Hz) electric field accompanying a SAW, with charge carriers in the film. Non-Arrhenius temperature behavior of the film conductivity measured by the SAW technique suggests that the charge carriers do not accumulate in grain boundary regions in the electric field of such high frequency and, hence, the screening of the applied electric field accompanying the SAW by the space charge, is negligible. Therefore, charge carrier transport in the SAW electric field is insensitive to the presence of the intergrain barriers, and the ohmic losses are fully determined by the conduction mechanism within the grains. As a result, using the SAW technique, we, in fact, measure the conductivity $\sigma(\omega, T)$ of the 2D polycrystal mentioned above formed by randomly oriented grains with *short-circuited* intergrain barriers. This conductivity can be represented as $\sigma(\omega, T) = \langle\sigma(T)\rangle + \sigma_p(\omega, T)$, where the first term is the dc conductivity of the 2D polycrystal and the second one is its ac conductivity, which is an isotropic value, calculated within the pair approximation. The problem of calculating the dc conductivity $\langle\sigma\rangle$ was solved by Dykhne [12]. He found that $\langle\sigma\rangle$ can be expressed as a formula of the principal values σ_{11} and σ_{22} of the intragrain conductivity tensor: $\langle\sigma\rangle = \sqrt{\sigma_{11}\sigma_{22}}$. Thus, it is the intragrain conductivity averaged over all possible grain orientations which is measured using the SAW attenuation technique, therefore, the temperature dependences of the conductivity obtained with this technique (data set 1, Fig. 1) point to the peculiarities of charge transport in the film grains.

To determine explicit expressions for σ_{11} and σ_{22}, it is necessary to consider intragrain carrier transport at the microscopic level. The inset (b) of Fig. 1 shows schematically the layered structure of the sample studied. The thicknesses of the insulating and conducting bilayers ($H \approx 25$ Å and $h \approx 10$ Å, respectively) were measured by electron diffraction technique. The in-plane structure of the conducting layer (see Fig. 2a) was schematically presented in Ref. [13]. Based on this work, we depicted the structure of the conducting bilayer in Fig. 2b. As can be seen, DMTTF and TCNQ head groups in the layer are arranged in separate stacks (chains) like molecular packing in TTF–TCNQ bulk crystals. However, the distance between neighboring DMTTF and TCNQ stacks in the layer is $a^{LB} \approx 7.65$ Å and the stacking distance within the TCNQ chain in the film is $b^{LB} \approx 4.76$ Å, while the similar distances in TTF–TCNQ crystals are $a^{cryst}/2 \approx 6.8$ Å and $b^{cryst} \approx 3.8$ Å, respectively [14]. Charge carrier transport in the conducting bilayers occurs mainly along the DMTTF and TCNQ stacks, as in the bulk parent crystals. Sometimes the carriers undergo hops between neighboring similar stacks. In other words, the system under consideration is a Q1D one. Negative sign of the Hall constant observed in Ref. [11] points out that the charge carriers in the film, like in TTF–TCNQ bulk crystals, propagate mainly along the TCNQ acceptor stacks. It should be noted that the distance between nearest TCNQ stacks in the bilayer is $a_\perp^{LB} = \sqrt{(h/2)^2 + (a^{LB})^2} \approx 9.2$ Å (see Fig. 2b). This value coincides practically with the distance between

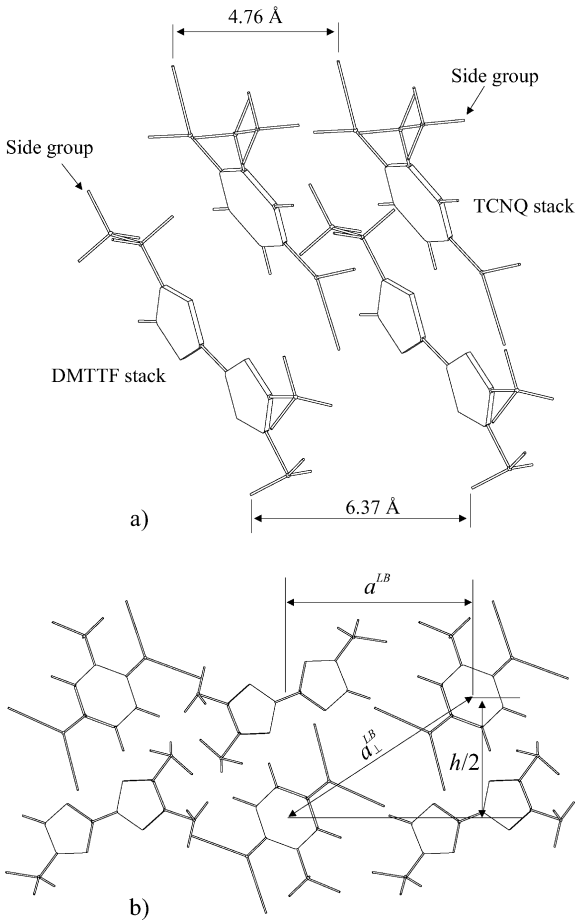

Fig. 2. (a) Schematic representation of the in-plane structure of the conducting layer. For clarity, only small fragments of the side groups ($-C_nH_{2n+1}$, $n = 16, 17$) are shown. The stacking distances within the TCNQ and DMTTF chains are taken from Ref. [13]. (b) The structure of the conducting bilayer. The axes of the TCNQ and DMTTF stacks are perpendicular to the plane of sketching. $a^{LB} \approx 7.65$ Å (taken from Ref. [13]), $h/2 \approx 5$ Å, $a_\perp^{LB} = \sqrt{(h/2)^2 + (a^{LB})^2} \approx 9.2$ Å.

nearest TCNQ stacks in TTF–TCNQ crystals [14]: $a_\perp^{cryst} = c^{cryst}/2 \approx 9.1$ Å.

Because of the intragrain electron transport anisotropy, the dc conductivity of the 2D grain as the whole is characterized by 2×2 tensor σ_{ij}. One of the principal axes of the tensor is parallel to the TCNQ stacks, the other axis is orthogonal to them. In the principal axes frame, the tensor has a diagonal form $\sigma_{ij} = \sigma_{ik}\delta_{kj}$, where δ_{kj} is the unit tensor, and $\sigma_{11} = \sigma_\parallel$, $\sigma_{22} = \sigma_\perp$ are the conductivities along the TCNQ stacks and in transverse direction to them, respectively.

It has been already mentioned above, the charge carriers propagate mainly along the TCNQ stacks. Impurities and defects in the stacks cause the scattering of electron waves with scattering intensity characterized by the relaxation time τ. Quantum interference of scattered electron waves results in electron localization accompanied by changing the

character of the Q1D DS conductivity, as well as decreasing its value. On the contrary, the interaction between individual TCNQ stacks with the intensity characterized by the transfer integral $t_\perp$, favors delocalization. The competition between these opposite tendencies leads to the possibility of the Q1D DS being in either metallic or insulating state, depending on the relation between $t_\perp$ and $\hbar/\tau$. It should be noted that inelastic scattering of electrons by phonons with wide enough energy dispersion (the intensity of such scattering is characterized by the electron–phonon relaxation time τ_{in}) also weakens the electron localization effects. Moreover, in the case when the condition $\tau_{in} \ll \tau$ is realized, a complete suppression of the electron localization is achieved, as it has been shown in Ref. [15]. It was found [16] that the considered Q1D DS undergoes a metal–insulator transition at $t_\perp \tau/\hbar = 0.3$. When $t_\perp > 0.3\hbar/\tau$, the system is in metallic state. When the opposite condition $t_\perp < 0.3\hbar/\tau$ is realized, the system is in nonmetallic state. The systematic study of the conductivity of the Q1D DS was carried out in Ref. [9] for various relations between $t_\perp$ and $\hbar/\tau$. Explicit expressions for $\sigma_\parallel(T)$, $\sigma_\perp(T)$ and $\sigma_p(\omega, T)$ derived in this reference will be used for fitting our experimental data (data set 1, Fig. 1) to the relation $\sigma(\omega, T) = \sqrt{\sigma_\parallel(T)\sigma_\perp(T)} + \sigma_p(\omega, T)$ in order to obtain the parameters characterizing electron transport within the film grains.

As it is shown in Fig. 1, the intragrain conductivity of the film studied does not exhibit metallic character. Correspondingly, it is reasonable to use the relations for $\sigma_\parallel(T)$, $\sigma_\perp(T)$, and $\sigma_p(\omega, T)$ found in Ref. [9] for the case of nonmetallic conduction regime, for fitting our experimental data (data set 1 in Fig. 1). The expression for the conductivity $\sigma_\perp(T)$ in the case has the form:

$$\sigma_\perp = 2e^2 g(\epsilon_F) a_\perp^2 \nu_{ph} (t_\perp \tau/\hbar)^2 \exp[-(T_0/T)^{1/2}], \quad (1)$$

where e is the electron charge, $g(\epsilon_F) = 1/(\pi\hbar v_F a_\perp^2)$ is the density of states with one sign of spin at the Fermi level, v_F is the Fermi velocity, $a_\perp$ is the distance between nearest chains, $\hbar$ is the Planck constant divided by 2π, $T_0 = 2\pi\hbar/(z k_B \tau)$, z is the number of nearest-neighboring chains [in our case, $z = 2$ (see Fig. 2b)], k_B is the Boltzmann constant, $\nu_{ph} = 1/\tau_{in}$.

Relation for $\sigma_\parallel$ obtained in original work [9] has a very bulky form. Based on the results of paper [9], Wang et al. [10] suggested more compact and convenient relation for $\sigma_\parallel$:

$$\sigma_\parallel = \frac{(4 v_F \tau) e^2 \nu_{ph}}{k_B T z a_\perp^2} (t_\perp \tau/\hbar)^2 \exp[-(T_0/T)^{1/2}]. \quad (2)$$

Expression for σ_p has the form [10]:

$$\sigma_p = \frac{(4 v_F \tau)^3 e^2 N(\epsilon_F)^2}{96} a_\perp^2 k_B T \omega \ln^2(\nu_{ph}/\omega), \quad (3)$$

where $N(\epsilon_F) = 2g(\epsilon_F)$.

It is evident that the net relation for the conductivity, $\sigma(\omega, T)$, depends on four parameters: $g(\epsilon_F)$, $t_\perp$, ν_{ph}, and T_0. The first two of these quantities can be estimated from the structural parameters of the bilayer shown in Fig. 2. Remaining parameters can be in turn extracted from the fitting of the expression for $\sigma(\omega, T)$ to our experimental data.

The interchain transfer integral, $t_\perp$, characterizes intensity of electron tunneling between neighboring TCNQ chains and decreases exponentially with increasing the interchain distance, $a_\perp$. As mentioned above, the distance between neighboring TCNQ chains in the film bilayer, $a_\perp^{LB}$, coincides practically with the analogous distance in TTF–TCNQ crystals, $a_\perp^{cryst}$. Therefore, the interchain transfer integral in our films, $t_\perp^{LB}$, should coincide with the one in the crystals, $t_\perp^{cryst}$. According to the electron band-structure calculations for TTF–TCNQ crystals [17], $t_\perp^{cryst} \approx 15$ meV. Consequently, $t_\perp^{LB} \approx 15$ meV.

Using the structural parameters of the layer shown in Fig. 2a allows us to estimate the Fermi velocity, v_F, and density of states, $g(\epsilon_F)$, in the film. Indeed, since $v_F \propto b t_\parallel$ (here $t_\parallel$ is the intrachain transfer integral, and b is the stacking distance in the chain), so $v_F^{cryst}/v_F^{LB} = b^{cryst} t_\parallel^{cryst}/(b^{LB} t_\parallel^{LB})$. The value of $t_\parallel^{cryst}$ is quoted in Ref. [18] to be $t_\parallel^{cryst} = 135$ meV, the values of b^{cryst} and b^{LB} have been mentioned above, hence it is necessary to calculate $t_\parallel^{LB}$. Similarly $t_\perp$, $t_\parallel$ also exponentially decays with increasing the distance, u, between neighboring TCNQ molecules in the stack. According to Ref. [10], $t_\parallel = Au \exp(-u/r_0)$. The constants A and r_0 can be easily evaluated from the following conditions: $t_\parallel|_{u=u^{cryst}} = t_\parallel^{cryst}$ and $\partial t_\parallel/\partial u|_{u=u^{cryst}} = -0.20$ eV/Å [19] (here $u^{cryst} = b^{cryst} \cos\theta = 3.17$ Å [14], where θ is the angle between the stack direction and the normal to the plane of the TCNQ molecule). Assuming the angle θ in the film has the same value as θ in TTF–TCNQ crystals, we get $u^{LB} = b^{LB} \cos\theta = 3.95$ Å. After simple calculations we obtain $t_\parallel^{cryst}/t_\parallel^{LB} \approx 3.176$, so that $t_\parallel^{LB} \approx 42.5$ meV, and $v_F^{cryst}/v_F^{LB} \approx 2.55$. The value of the Fermi velocity in TTF–TCNQ crystals is cited in Ref. [19] to be $v_F^{cryst} \approx 1.2 \times 10^7$ cm/s, hence $v_F^{LB} \approx 4.7 \times 10^6$ cm/s. We have pointed out above that $a_\perp^{LB} \approx a_\perp^{cryst}$, thus $g^{LB}(\epsilon_F)/g^{cryst}(\epsilon_F) \approx v_F^{cryst}/v_F^{LB} \approx 2.55$. Since $g^{cryst}(\epsilon_F)$ is known to be $g^{cryst}(\epsilon_F) \approx 4.7 \times 10^{21}$ eV^{-1} cm^{-3} [20], so $g^{LB}(\epsilon_F) \approx 1.2 \times 10^{22}$ eV^{-1} cm^{-3}.

In Refs. [9,15] it was noted that the temperature dependence of $\nu_{ph} = 1/\tau_{in}$ has a different behaviour for temperatures above and below Debye's temperature, Θ_D, of the considered system: in the case when $T > \Theta_D$, $\tau_{in}^{-1} \propto T$, and in the opposite case when $T < \Theta_D$, $\tau_{in}^{-1} \propto T^3$. Debye's temperature of DMTTF–TCNQ crystals was determined in Ref. [21] to be $\Theta_D^{cryst} \approx 85$ K. Below we present some arguments in favor of statement that Θ_D^{LB} of our LB films is not greater than Θ_D^{cryst} at least. Indeed, as we have pointed out above, the distance between neighboring DMTTF and TCNQ chains in the layer, as well as the distance between nearest neighbors in the chain, are larger than corresponding distances in the bulk parent crystals. Moreover, the presence of the dielectric layers, formed by hydrocarbon side groups [see inset (b) of Fig. 1], significantly reduces the interaction between separate conducting bilayers. As a result,

conducting LB films are more 'soft' systems than corresponding crystalline materials and, hence, $\Theta_D^{LB} \leq \Theta_D^{cryst}$. Therefore we should assume that $\nu_{ph} = 1/\tau_{in} \propto T$ over the whole temperature range (100 K $< T <$ 300 K) studied.

In order to describe quantitatively the temperature dependence of τ_{in}^{-1} for TTF–TCNQ crystals, Bright et al. [22] proposed to use the Hopfield relation: $\tau_{in}^{-1}(T) = 2\pi k_B T\lambda/\hbar$, where λ is a dimensionless electron–phonon interaction constant. Berlinsky [23] found that $\lambda \approx 0.23$ for TTF–TCNQ crystals. While fitting the theoretical dependence $\sigma(\omega, T)$ (see Eqs. (1)–(3)) to our experimental data (data set 1 of Fig. 1) we also assume that $\nu_{ph}(T) = 2\pi k_B T\lambda/\hbar$. Since the value of the electron–phonon interaction constant λ for LB films studied is unknown, we consider the parameter λ as an adjustable one, whose value has to be determined from the fitting procedure.

Finally, the parameter T_0 occurring in Eqs. (1) and (2), and related to the electron relaxation time due to scattering by impurities, is also assumed as an adjustable parameter whose value should be obtained from the fitting.

Fixing $t_\perp = 15$ meV, $g(\epsilon_F) = 1.2 \times 10^{22}$ eV^{-1} cm^{-3} and varying T_0 and λ we have fitted the relation $\sigma(\omega, T) = \sqrt{\sigma_\parallel(T)\sigma_\perp(T)} + \sigma_p(\omega, T)$ to our experimental data. The fitting procedure gives $T_0 = 5035 \pm 240$ K, and $\lambda = 0.18 \pm 0.04$. The values of the best-fit parameters T_0 and λ were found to be insensitive to their starting values. The solid line in Fig. 3 shows the best fit with $\sigma(\omega, T)$ relation. Using Eqs. (1)–(3) and the obtained values of T_0 and λ we calculated the temperature dependences of $\sigma_\parallel(T)$, $\sigma_\perp(T)$ and $\sigma_p(\omega, T)$. They are represented by the dashed curves (a)–(c), respectively, in Fig. 3. As can be seen, $\sigma_\parallel(T) \approx \sigma_\perp(T) \gg \sigma_p(\omega, T)$ at room temperature, whereas at low temperature $\sigma_\parallel(T) > \sigma_\perp(T) \approx \sigma_p(\omega, T)$. From the found value of T_0 we determined the electron relaxation time due to scattering by impurities: $\tau = 4.8 \times 10^{-15}$ s. Using this time together with value of the Fermi velocity obtained above we calculated the mean free path $l = v_F^{LB}\tau \approx 0.5b^{LB}$ and the localization length $l_{loc} = 4l$ [15]: $l_{loc} = 4v_F^{LB}\tau \approx 9.0$ Å. It is seen that the localization length in the film is less than the double stacking distance within the chain.

It is interesting to compare the obtained values of l and τ with analogous parameters of the systems in which the electron localization effects play an important role. The best-known examples of such systems are conducting polymers and structurally disordered 1:2 complexes of quinolinium (Qn) and acridinium (Ad) with TCNQ, $Qn(TCNQ)_2$ and $Ad(TCNQ)_2$, respectively. In polypyrrole doped with hexafluorophosphate (PF_6), τ and l were found to be 5.5×10^{-16} s and $0.85a$, respectively [24] (a denotes the length of the structural repeat unit along the polymer chain). Similar parameters for $Qn(TCNQ)_2$ were reported in Ref. [25] to be 1.3×10^{-14} s and $2.5b$, respectively (b means the lattice spacing along the TCNQ chain). As can be seen, our LB films stay between conducting polymers and TCNQ salts with asymmetric cations with respect to degree of electron localization in them.

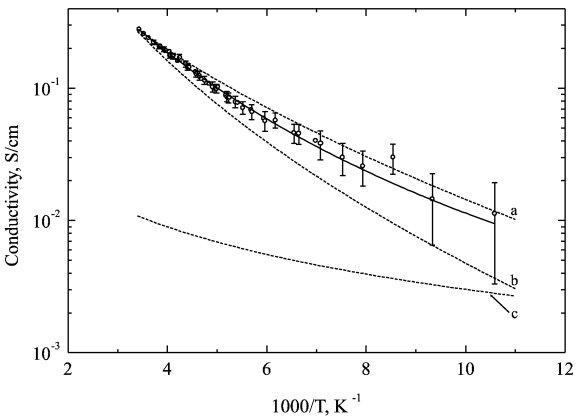

Fig. 3. The experimental data of Fig. 1 (data set 1). The solid line represents the best fit with theoretical relation $\sigma(\omega, T) = \sqrt{\sigma_\parallel(T)\sigma_\perp(T)} + \sigma_p(\omega, T)$, where $\sigma_\parallel(T)$, $\sigma_\perp(T)$ and $\sigma_p(\omega, T)$ are defined by Eqs. (1)–(3). The best fit to the data is obtained for $T_0 = 5035$ K and $\lambda = 0.18$. The T dependences of $\sigma_\parallel(T)$, $\sigma_\perp(T)$ and $\sigma_p(\omega, T)$ calculated using the best-fit values of T_0 and λ are represented by the dashed curves (a)–(c), respectively. $\omega = 2\pi 87.9$ MHz.

It is a common practice to make conclusions about the electron localization strength by comparing the value of $k_F l$ (where k_F is the Fermi wave vector) with 1. The value of $k_F l \leq 1$ indicates that a strong (Anderson-type) localization takes place, and in the opposite case ($k_F l \gg 1$) it indicates that a weak localization is realized. For the considered LB films $k_F l = \pi\rho l/b^{LB}$, where ρ is the degree of charge-transfer from donor to acceptor. Assuming that ρ of our LB films is the same as one of corresponding bulk TTF–TCNQ crystals ($\rho \approx 0.6$) we obtain that $k_F l \approx 0.9$. This fact points to a strong localization in our LB films.

Using the value of λ obtained from the fitting procedure, we calculated the value of the electron–phonon relaxation time at room temperature: $\tau_{in}(294\text{ K}) = 2.3 \times 10^{-14}$ s. As can be seen, $\tau_{in}(294\text{ K}) > \tau$. It was already mentioned above that electron–phonon inelastic scattering suppresses the localization effects. For example, in TTF–TCNQ crystals because of their high purity and strong electron–phonon interaction in them, the inequality $\tau_{in}^{cryst} \ll \tau^{cryst}$ holds. This leads to complete suppression of the electron localization and metallic character of the conductivity of the crystals (above the Peierls transition temperature), in spite of its quasi-one-dimensional structure [9]. As shown in Fig. 3, the conductivity of our films is not metallic ($\partial\sigma/\partial T > 0$). This fact can be explained by a higher number of impurities and defects in their structure in comparison with TTF–TCNQ crystals, resulting in the inequality $\tau^{LB} \ll \tau^{cryst}$. Because of this, the inelastic scattering is unable (according to the relation $\tau_{in}^{LB} > \tau^{LB}$) to destroy electron wave interference, resulting in the localization which determines the observed nonmetallic character of the film conductivity. In this connection, one should note that if we could increase τ^{LB} by order of magnitude (by improving purity of the films

and reducing the number of defects in them), then for a certain temperature range the relation $\tau_{in}^{LB} \ll \tau^{LB}$ would be fulfilled and a metallic conductivity of the film ($\partial\sigma/\partial T < 0$) might be realized. A similar phenomenon was observed by Shchegolev's group [25] in the bulk TCNQ salts mentioned above with intrinsic structural disorder due to cation asymmetry. For example, below 240 K Qn(TCNQ)$_2$ crystals exhibit the nonmetallic conductivity, $\sigma \propto \exp(-1/T^{1/2})$, originating from localization of the electron states in TCNQ stacks. But in the temperature range 240 K $< T <$ 300 K, the metallic conductivity of the crystals ($\partial\sigma/\partial T < 0$) is observed because of suppression of the electron localization by electron–phonon inelastic scattering.

It has been already mentioned above that the LB films of the mixture of BEDO-TTF with fatty acids have the highest conductivity among the films of charge-transfer complexes. Recently in the LB films of the mixture of BEDO-TTF with stearic acid (SA) Ishizaki et al. [26] have found the negative magnetoresistance, which was explained by them in terms of weak electron localization. It is important to note in this connection that electron localization in our LB films is stronger in comparison with the films of the mixture of BEDO-TTF and SA, whose conductivity exhibits a metallic character at temperatures down to 120 K and weakly logarithmically decreases with lowering temperature below 120 K. We explain the difference in their degree of localization by strong interaction between BEDO-TTF molecules within conducting layers of the BEDO-TTF + SA films, resulting in formation of a quasi-two-dimensional (Q2D) electron system. In other words, the charge carriers in these films propagate along the conducting layers, whereas, in the case of our LB films, electrons move along the Q1D stacks. It is well known that the localization effects are much more pronounced in Q1D systems than in Q2D one under the same defects and impurities concentrations.

In conclusion, in the paper we presented results of a study of the temperature dependence of the intragrain conductivity of the LB films of $(C_{16}H_{33}–TCNQ)_{0.4}(C_{17}H_{35}–DMTTF)_{0.6}$ charge-transfer complex, measured using the SAW attenuation technique, proposed by us previously in Ref. [8]. The intragrain conductivity was found to follow $\sigma \propto \exp(-1/T^{1/2})$ law, indicating that the electron states in the TCNQ chains within the film grains are localized. The observed temperature dependence of the conductivity was in qualitative and quantitative agreement with the predictions of the theory of electron localization in Q1D DS proposed in Ref. [9] and developed in Ref. [10]. Fitting the theoretical relations derived in these references to our experimental data allowed us to evaluate the electron–phonon relaxation time at room temperature, and the electron relaxation time due to scattering by impurities, $\tau_{in}(294\ \mathrm{K}) = 2.3 \times 10^{-14}$ s and $\tau = 4.8 \times 10^{-15}$ s, respectively. Based on the structural parameters of the conducting bilayer, we also estimated the Fermi velocity ($v_F^{LB} \approx 4.7 \times 10^6$ cm/s) and the density of states at the Fermi level [$g^{LB}(\epsilon_F) \approx 1.2 \times 10^{22}$ eV^{-1} cm^{-3}], which allowed us to determine the mean free path, l, and the localization length, l_{loc}, in the film studied: $l_{loc} = 4l = 4v_F^{LB}\tau \approx 9.0$ Å.

Acknowledgements

This work was supported by the Russian Foundation for Basic Research (grants no. 01-02-16068, 00-02-22000) and by the President Program of Support for the Leading Scientific Schools (grant no. 1391.2003.2).

References

[1] P. Delhaés, V.M. Yartsev, in: R.J.H. Clark, R.E. Hester (Eds.), Spectroscopy of New Materials, vol. 22, Wiley, Chichester, 1993, p. 199.
[2] T. Nakamura, et al., J. Phys. Chem. 98 (1994) 1882.
[3] H. Ohnuki, et al., Phys. Rev. B 55 (1997) R10225.
[4] S. Kahlich, et al., Solid State Commun. 80 (1991) 191.
[5] J. Richard, et al., J. Phys. D: Appl. Phys. 19 (1986) 2421.
[6] I.F. Shchegolev, Phys. Stat. Solidi A 12 (1972) 9.
[7] H.W. Helberg, M. Dressel, J. Phys. I France 6 (1996) 1683.
[8] V. Chernov, et al., Solid State Commun. 97 (1996) 49.
[9] E.P. Nakhmedov, et al., Fiz. Tverd. Tela. (Leningrad) 31 (1989) 31 [Sov. Phys. Solid State 31 (1989) 368].
[10] Z.H. Wang, et al., Phys. Rev. B 43 (1991) 4373.
[11] L.A. Galchenkov, et al., Synth. Met. 42 (1991) 1471.
[12] A.M. Dykhne, Zh. Eksp. Teor. Fiz. 59 (1970) 110 [Sov. Phys. - JETP 32 (1970) 63].
[13] F. Rustichelli, et al., Thin Solid Films 242 (1994) 267.
[14] T.J. Kistenmacher, et al., Acta Crystallogr. B30 (1974) 763.
[15] A.A. Gogolin, et al., Zh. Eksp. Teor. Fiz. 69 (1975) 327 [Sov. Phys. - JETP 42 (1975) 168].
[16] V.N. Prigodin, Y.A. Firsov, Pis'ma Zh. Eksp. Teor. Fiz. 38 (1983) 241 [JETP Lett. 38 (1983) 284].
[17] S. Ishibashi, M. Kohyama, Phys. Rev. B 62 (2000) 7839.
[18] D. Jérome, H.J. Schulz, Adv. Phys. 31 (1982) 299.
[19] E.M. Conwell, Phys. Rev. B 22 (1980) 1761.
[20] S.K. Khanna, et al., Phys. Rev. B 10 (1974) 2205.
[21] T. Wei, et al., Phys. Rev. B 20 (1979) 5090.
[22] A.A. Bright, A.F. Garito, A.J. Heeger, Phys. Rev. B 10 (1974) 1328.
[23] A.J. Berlinsky, Contemp. Phys. 17 (1976) 331.
[24] K. Lee, et al., Phys. Rev. B 52 (1995) 4779.
[25] A.A. Gogolin, et al., Pis'ma Zh. Eksp. Teor. Fiz. 22 (1975) 564 [JETP Lett. 22 (1975) 278].
[26] Y. Ishizaki, et al., Phys. Rev. B 63 (2001) 134201.